Supporting Information

Yin et al. 10.1073/pnas.1400667111

SI Text

Optical Setup. The fluorescence correlation spectroscopy (FCS) experiments were performed using Nikon TE2000 inverted fluorescence microscopy system (1). The illumination beam was provided by a 532-nm continuous-wave Ya–Ge Laser (SUW Tech) and focused into the sample solution through a 100× N.A. 1.4 oil-immersion objective (Nikon). We kept the laser power at 20 μW before entering the objective to minimize the triplet state formation and photo bleaching. The emitted fluorescence was separated from the illumination beam by a CY3 dichroic filter (Chroma Tech) and further spectrally filtered by a bandpass 593/40 filter (Semrock). We applied a 30-μm pinhole to spatially filter the emitted photons. The fluorescence signal was 50:50 split and then collected by two avalanched photodiodes (SPCM-AQR-14, PerkinElmer) for the cross-correlation so as to avoid the after pulsing in the autocorrelation.

FCS Measurement. The sample solution was put in a chamber (GraceBio, Sigma) sealed by cover glasses which were prepared using piranha solution for more than 60 min at above 90 °C. Both the conventional FCS and diffusion-decelerated FCS (ddFCS) measurements were taken in a plane ∼10 μm above the cover glass surface. In the conventional FCS experiments, the measurement took 1 h for each sample and the correlation was in situ calculated using a computer-implemented correlator (Flex 02–01D, www.correlator.com). For the ddFCS experiments, the fluorescence traces were recorded every 60 s and we selected traces that contained the event to calculate the correlation. More than 80 events were collected for each measurement to guarantee the convergence (1). The concentration of the dsDNA was 10 nM for the conventional FCS and 0.1% of the microspheres for the ddFCS measurements, respectively. Both the dsDNA and the DNA–microsphere complex were in the buffer composed of 10 mM Tris·HCl and 1 mM EDTA with pH = 8.5, and [NaCl] = 300 mM.

Steady-State Fluorescence Experiment. The steady-state fluorescence experiments were carried out on a Renishaw1000 microscopic spectrometer (Britain) equipped with a continuous-wave Ya–Ge laser (532 nm) (SUW Tech) for illumination. The temperature was controlled by using a THMS600 temperature controller, by which the samples were heated from 4 °C to 80 °C at a speed of 2 °C/min. The melting curves given in Figs. 1*C* and 3*B* were obtained by accumulating the collected fluorescence intensities from 579–589 nm about every 5 s with the evenly increasing temperature. Because the respective dsDNA molecules had the same tetramethylrodamine (TMR)-labeled ssDNA (Table S1), the curves were linearly scaled according to the data from 70 °C to 80 °C after the dsDNAs were melted, to correct the concentration factor. The concentration of the dsDNA was 10 nM in the buffer composed of 10 mM Tris·HCl and 1 mM EDTA with pH = 8.5, and [NaCl] = 300 mM.

Steady-State Fluorescence Anisotropy Experiment. The steady-state fluorescence anisotropy experiments were carried out on a spectrofluorophotometer (RF-5301PC, Shimadzu) equipped with its built-in polarizer (P/N 204–03290-01). Both the excitation and emission polarizer can be oriented between vertical and horizontal directions, enabling us to collect the fluorescence with different combinations of excitation and emission polarizations. The fluorescence intensities were recorded as $I_{EX/EM}$, where both the EX (Excitation) and EM (Emission) can be V (Vertical) or H (Horizontal). The transmission efficiency of the apparatus in different orientations was corrected by the factor $k = I_{HV}/I_{HH}$, and the anisotropy is calculated by $r = (I_{VV} - kI_{VH})/(I_{VV} + 2kI_{VH})$ (Fig. S3). The concentration of the dsDNA was 100 nM in the buffer composed of 10 mM Tris·HCl and 1 mM EDTA with pH = 8.5, and [NaCl] = 300 mM, and all of the anisotropy experiments were performed at 25.0 ± 1.0 °C.

Oligonucleotide Synthesis. The oligonucleotides labeled with TMR were made by incorporating the N^4-6-TMR-dC-CE phosphoramidite (Chemgenes) at the desired position during solid-phase synthesis (2). The synthetic oligonucleotides were purified with denaturing polyacrylamide gelelectrophoresis. The ssDNAs containing O^6meG were purchased from Takara and other oligonucleotides without modification or label were purchased from Sangon Biotechnique, all with HPLC purification. All of the dsDNAs in Table S1 were hybridized from two ssDNAs by mixing and incubating at 90 °C for 5 min and then slowly cooling down to room temperature for reannealing.

ddFCS Data Processing. As mentioned in the *Extraction of Dynamic and Thermodynamic Parameters from Obtained ddFCS Data* subsection of the main text, the experimentally recorded correlation function of the mismatch-containing dsDNA (the G–T or C–T and T–T mismatch), G_{MM}, was divided by the experimentally recorded correlation function of the perfectly matched dsDNA (the G–C or A–T match), G_{WC}, to remove the correlation from diffusion. The remaining correlation due to the base flipping is given by (3)

$$G_{\text{flip}}(\tau) = \frac{G_{MM}(\tau)}{G_{WC}(\tau)} = 1 + \alpha \exp\left(-\frac{\tau}{\tau_{\text{flip}}}\right) = 1 + \frac{K(1-Q)^2}{(1+KQ)^2} \exp\left[-\left(k_{\text{flip-out}} + k_{\text{flip-in}}\right)\tau\right], \quad \textbf{[S1]}$$

where K is the equilibrium constant of the reaction from the fluorescent state to the dark state, Q is the ratio of brightness of the dark state over the fluorescent state, $k_{\text{flip-out}}$ and $k_{\text{flip-in}}$ are the out- and inward base flipping rate constants, respectively. $G_{\text{flip}}(\tau)$ was fitted by a single-exponential decay function using the nonlinear least-squares Marquardt algorithm to determine α and τ_{flip}. Notably, for the T–T and C–T mismatches the K derived from Eq. **S1** is the equilibrium constant of base-pair opening (i.e., $K = K_{\text{open}} = k_{\text{flip-out}}/k_{\text{flip-in}}$) because the dark state corresponds to the flipped-out state (Fig. 3 *A* and *B*), whereas for the G–T mismatch the K derived from Eq. **S1** should be the equilibrium constant of base-pair closing (i.e., $K = K_{\text{close}} = 1/K_{\text{open}}$) because the dark state corresponds to the flipped-in state (Fig. 1 *A* and *C*). We report K_{open} for all of the T–T, C–T, and G–T mismatches, which are derived to be

$$K_{\text{open}}^{(\text{G-T})} = \left[\frac{(1-Q)^2 - 2\alpha Q + (1-Q)\sqrt{(1-Q)^2 - 4\alpha Q}}{2\alpha Q^2}\right]^{-1}, \quad \textbf{[S2]}$$

$$K_{\text{open}}^{(\text{T/C-T})} = \frac{(1-Q)^2 - 2\alpha Q - (1-Q)\sqrt{(1-Q)^2 - 4\alpha Q}}{2\alpha Q^2}, \quad \textbf{[S3]}$$

where

$$K_{\text{open}} = \frac{k_{\text{flip-out}}}{k_{\text{flip-in}}}. \quad \textbf{[S4]}$$

Our previous study showed that $Q = 0.1$ for the TMR-G photoinduced electron transfer (PET) pair (3), and this value was taken here to calculate K. In fact, the variation of Q in a wide range causes little change on K owing to the small probability of the spontaneous outward flipping for all of the G–T, T–T, and C–T mismatches (Fig. S5). Fitting experimentally observed G_{flip} by Eqs. **S1**–**S4**, $k_{\text{flip-out}}$ and $k_{\text{flip-in}}$ as well as K_{open} were obtained.

Details of Molecular Simulation. Selective integrated tempering sampling (SITS) was applied to calculate the individual potentials of mean force for the flipping of the mismatched G or T bases in the dsDNA used for the simulation (dodecamer, Table S1). The canonical B form of the dsDNA was solvated in a rectangular simulation box which contains 3,606 simple point charge (SPC) water molecules. Twenty sodium ions were added to neutralize the simulation system. Nucleic acid force-field parameters were taken from the AMBER (Assisted Model Building with Energy Refinement) ff10 parameter set (4). The SHAKE (5) algorithm with a relative geometric tolerance of 10^{-8} Å was used to constrain all covalent bonds including hydrogen. Thus, all dynamics used a 2-fs time step. Long-range electrostatics was treated by the particle-mesh Ewald (6) method with default settings. The aqueous system was first subjected to 1,000 steps of steepest descent energy minimization, followed by 1,000 steps of conjugate gradient optimization. Then, a 100-ps molecular dynamics simulation was performed with the temperature adjusted to 300 K by the Langevin dynamics with a friction coefficient of 1 ps^{-1}. To equilibrate the system to the appropriate volume, the pressure of the system was then adjusted to 1 atm by the Berendsen weak-coupling (7) algorithm with the relaxation time constants of 2.0 ps in another 1-ns molecular dynamics simulation. Starting from the equilibrated state, SITS simulations were carried out using a modified SANDER program from the AMBER9 molecular mechanics package (8). In SITS simulations, the system was divided into two subregions: the central group which contains only the flipping G or T base and the bath which includes all of the other bases, sodium ions, and water molecules. The system temperature was maintained at 300 K and 100β values evenly distributed from 280 to 600 K were selected to generate the effective potential (Eq. **S5**) for the enhanced sampling of the flipping of the G or T base:

$$U' = E_{\text{bath}} + \frac{1}{2}E_{\text{int}} - \frac{1}{\beta_0}\ln\sum_{k=1}^{N} n_k e^{-\beta_k\left(E_c+\frac{1}{2}E_{\text{int}}\right)}, \qquad \textbf{[S5]}$$

where E_c, E_{bath}, and E_{int} are the potential energies of the central group, the bath, and the interactions between the central group and the bath, respectively, and β_0 equals $1/(k_B T_0)$, where k_B is the Boltzmann constant and T_0 is the objective temperature. Firstly, a set of randomly selected n_k values was used to generate the bias potential. Then an iteration process (9) was applied to adjust the values of n_k until a uniformly efficient sampling in the desired energy range was achieved. After the values of n_k were determined, eight independent SITS simulations starting from different initial structures were conducted for G and T flipping, respectively. Each SITS simulation was executed for 100 ns and the configurations and energies were recorded every 1 ps.

The free-energy profile of flipping was calculated along the dihedral angle defined in Fig. 5*A* in 10° increments from −180° to 180°. The simulations in the presence of the bias potential allowed for all accessible conformations of the flipping base to be sampled, yielding a biased probability distribution. The probability distribution was then corrected by timing the reweighting factor $e^{\beta_0[U'(r)-U(r)]}$, yielding the unbiased probability distribution, $P(x)$, from which the free-energy surface was extracted via $\Delta G = -k_B T \ln P(x)$.

Some Remarks. Because we perform simulations under the effective potential (Eq. **S5**), we can easily obtain the thermodynamics of the system by a convenient reweighting process. The comparison between experiments and theory is thus made for thermodynamics. However, the real kinetic information has been lost in this kind of enhanced sampling simulation. Use of enhanced transition path sampling method which can offer kinetic information of the system should be explored to theoretically explain all kinetic details revealed experimentally. Why, for instance, is the energetics in Table S3 quite different among the mismatches? We cannot provide an explanation just now. The difference in H-bonding interaction, solvation, and stacking energies of thymine, cytosine, and guanine could be possible reasons. Previous studies show that the mismatch varies the stability of the helix with the degree of destabilization depending on the mismatched pair (10, 11) The differences in enthalpy and entropy of helix formation can be dramatic between different mismatched pairs and sequence environments (11), which certainly disturbs the helix formation and induces different behavior in base flipping.

We are now applying our methodology to investigate other important systems. One example is the spontaneous flipping of the O^6meG–T and O^6meG–C pairs. G to O^6meG is a lesion seen in organisms. It is reported that O^6meG–T and O^6meG–C could form one and two H bonds in physiological conditions, respectively (12, 13). Our measurement at 25 °C showed that indeed their equilibrium constants and lifetimes are in consistence with the expectation based on such possibilities (Table S2).

1. Yin Y, et al. (2012) Panorama of DNA hairpin folding observed *via* diffusion-decelerated fluorescence correlation spectroscopy. *Chem Commun (Camb)* 48(59): 7413–7415.
2. Mishina Y, He C (2003) Probing the structure and function of the Escherichia coli DNA alkylation repair AlkB protein through chemical cross-linking. *J Am Chem Soc* 125(29): 8730–8731.
3. Li X, Zhu R, Yu A, Zhao XS (2011) Ultrafast photoinduced electron transfer between tetramethylrhodamine and guanosine in aqueous solution. *J Phys Chem B* 115(19): 6265–6271.
4. Pérez A, et al. (2007) Refinement of the AMBER force field for nucleic acids: Improving the description of α/γ conformers. *Biophys J* 92(11):3817–3829.
5. Ryckaert JP, Ciccotti G, Berendsen HJC (1977) Numerical-integration of the Cartesian equations of motion of a system with constraints: Molecular-dynamics of n-alkanes. *J Comput Phys* 23(3):327–341.
6. Darden T, York D, Pedersen L (1993) Particle mesh Ewald: An *N*·log(*N*) method for Ewald sums in large systems. *J Chem Phys* 98(12):10089–10092.
7. Berendsen HJC, Postma JPM, van Gunsteren WF, Dinola A, Haak JR (1984) Molecular dynamics with coupling to an external bath. *J Chem Phys* 81(8):3684–3690.
8. Case DA, et al. (2006) AMBER 9 (University of California, San Francisco).
9. Gao YQ (2008) Self-adaptive enhanced sampling in the energy and trajectory spaces: Accelerated thermodynamics and kinetic calculations. *J Chem Phys* 128(13):134111.
10. Modrich P (1987) DNA mismatch correction. *Annu Rev Biochem* 56:435–466.
11. Aboul-ela F, Koh D, Tinoco I, Jr., Martin FH (1985) Base-base mismatches. Thermodynamics of double helix formation for $dCA_3XA_3G + dCT_3YT_3G$ (X, Y = A,C,G,T). *Nucleic Acids Res* 13(13):4811–4824.
12. Patel DJ, Shapiro L, Kozlowski SA, Gaffney BL, Jones RA (1986) Structural studies of the O6meG.T interaction in the d(C-G-T-G-A-A-T-T-C-O6meG-C-G) duplex. *Biochemistry* 25(5): 1036–1042.
13. Warren JJ, Forsberg LJ, Beese LS (2006) The structural basis for the mutagenicity of O(6)-methyl-guanine lesions. *Proc Natl Acad Sci USA* 103(52):19701–19706.

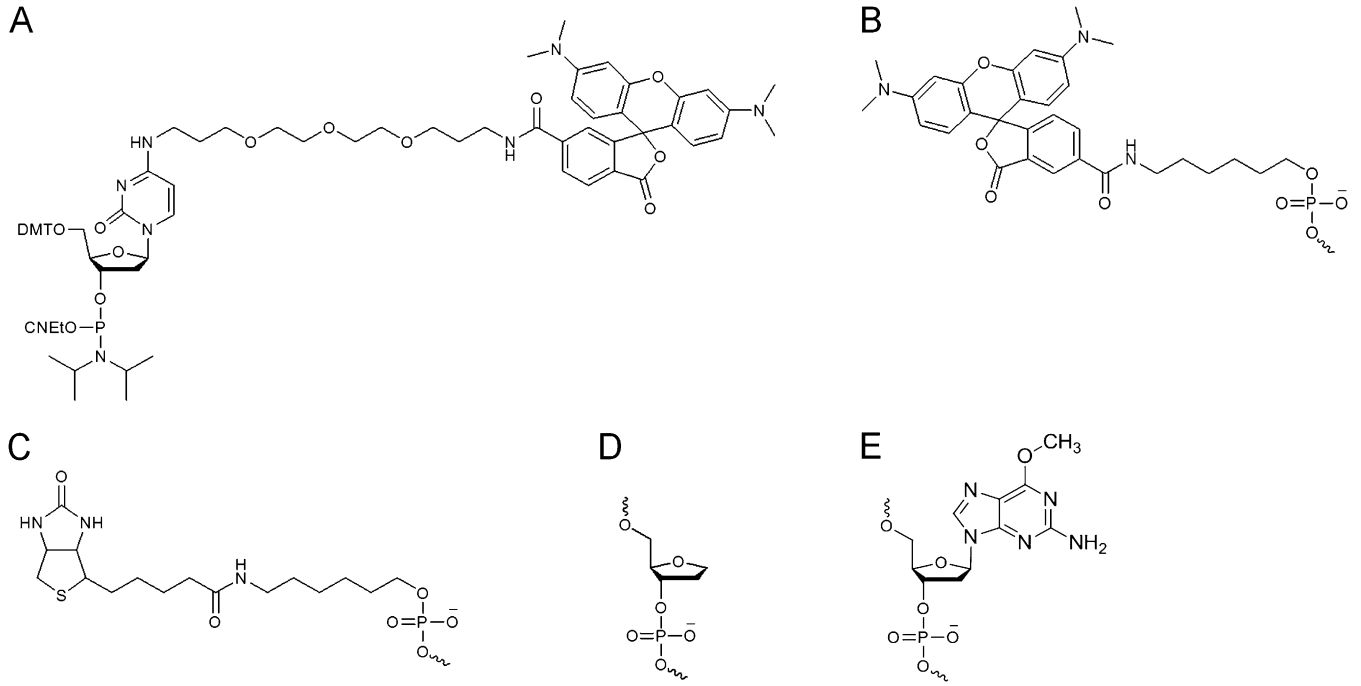

Fig. S1. Structures of TMR and biotin and their linkers used in this work. (*A*) Structure of N^4-6-TMR-dC-CE phosphoramidite (Chemgenes), which was incorporated at the desired position during solid-phase synthesis of the T–A match, T–C mismatch, T–G mismatch, T–T mismatch, C–G match, ssC, and ssT (Table S1). (*B*) Structure of TMR labeled at the 5′ end of the oligonucleotide used in TMR-termi (Sangon, Table S1). (*C*) Structure of biotin labeled at the 5′ end of ssC and ssT, and oligonucleotides used in the T–A match, T–C mismatch, T–G mismatch, T–T mismatch, and C–G match. (*D*) Structure of the abasic nucleotide used in the *N*–T mismatch (Table S1). (*E*) Structure of O^6meG used in the O^6meG–T and O^6meG–C pairs.

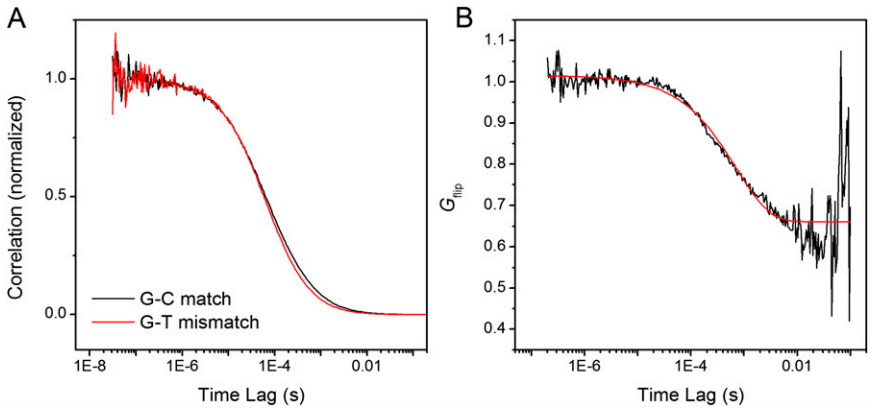

Fig. S2. (*A*) Conventional FCS data of the G–T mismatch (red) and the G–C match (black) at 25.0 ± 0.5 °C. Little difference was observed in millisecond order. (*B*) Ratio of curve of the G–T mismatch over that of the G–C match in *A* (black) and a stretched-exponential fit (red). If assuming that the decay was due to the base flipping, the average relaxation time of base flipping would be $\langle\tau\rangle = \tau_R \cdot \Gamma(\beta^{-1})/\beta = 0.90 \pm 0.01$ ms, where τ_R and β were obtained by the stretched-exponential fitting (1) and the error was propagated SE from the fit. The G_{flip} in the dashed box in *B* shows an unsatisfactory fit for the possible slow kinetic components.

1. Klafter J, Shlesinger MF (1986) On the relationship among three theories of relaxation in disordered systems. *Proc Natl Acad Sci USA* 83(4):848–851.

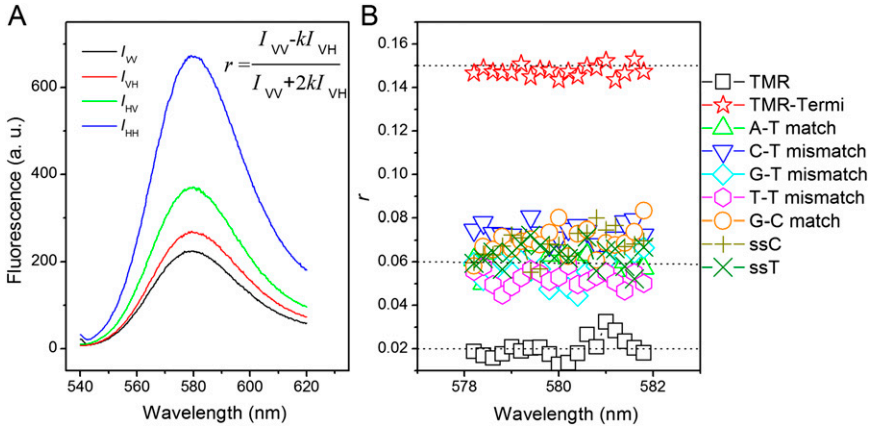

Fig. S3. Fluorescence anisotropy measurements indicated that the observed relaxation was not caused by the fluorescence labeling. (*A*) An example of fluorescence anisotropy measurements on TMR-termi at 25.0 ± 1.0 °C. We recorded the fluorescence intensities with different combinations of excitation and emission polarizations, $I_{EX/EM}$. The subscript V stands for vertical and H for horizontal. We calculated the fluorescence anisotropy according to the equation in the figure, where k is the correction factor for transmission efficiency of the apparatus in different orientations. (*B*) Fluorescence anisotropies of different samples. For the TMR-termi molecule, TMR was mostly capped on the end of the DNA duplex so that it rotates together with the dsDNA (1, 2). As a result, high fluorescence anisotropy was observed. The observed anisotropy for the A–T, G–C matches and G–T, T–T, C–T mismatches was much lower than TMR-termi and consistent with their single-stranded counterparts (ssC and ssT), indicating that the middle-labeled TMR-linker group swings much faster than that capped to the end of the duplex DNA (TMR-termi) and manifests lower anisotropy. Because the end-capped TMR-linker swings on the order of submicrosecond (3) and the middle-labeled dsDNAs swing faster, the TMR-linker motion does not cause the correlation decay on the order of ∼10 ms.

1. Unruh JR, Gokulrangan G, Lushington GH, Johnson CK, Wilson GS (2005) Orientational dynamics and dye-DNA interactions in a dye-labeled DNA aptamer. *Biophys J* 88(5):3455–3465.
2. Li X, Yin Y, Yang X, Zhi Z, Zhao XS (2011) Temperature dependence of interaction between double stranded DNA and Cy3 or Cy5. *Chem Phys Lett* 513:271–275.
3. Yin Y, et al. (2012) Panorama of DNA hairpin folding observed *via* diffusion-decelerated fluorescence correlation spectroscopy. *Chem Commun (Camb)* 48(59):7413–7415.

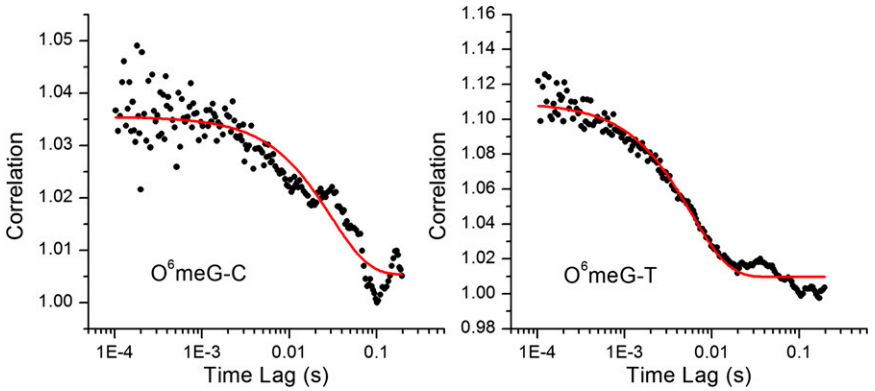

Fig. S4. Ratio of correlation by dividing the ddFCS curve of the O^6meG–C (*Left*) and O^6meG–T (*Right*) mismatches over that of the G–C match. All of the ddFCS data were taken at T = 25.0 ± 0.2 °C. The flipping rate and equilibrium constants, obtained through single-exponential decay fit of the curves, are listed in Table S2. Similar to G, O^6meG is a fluorescence quencher of TMR.

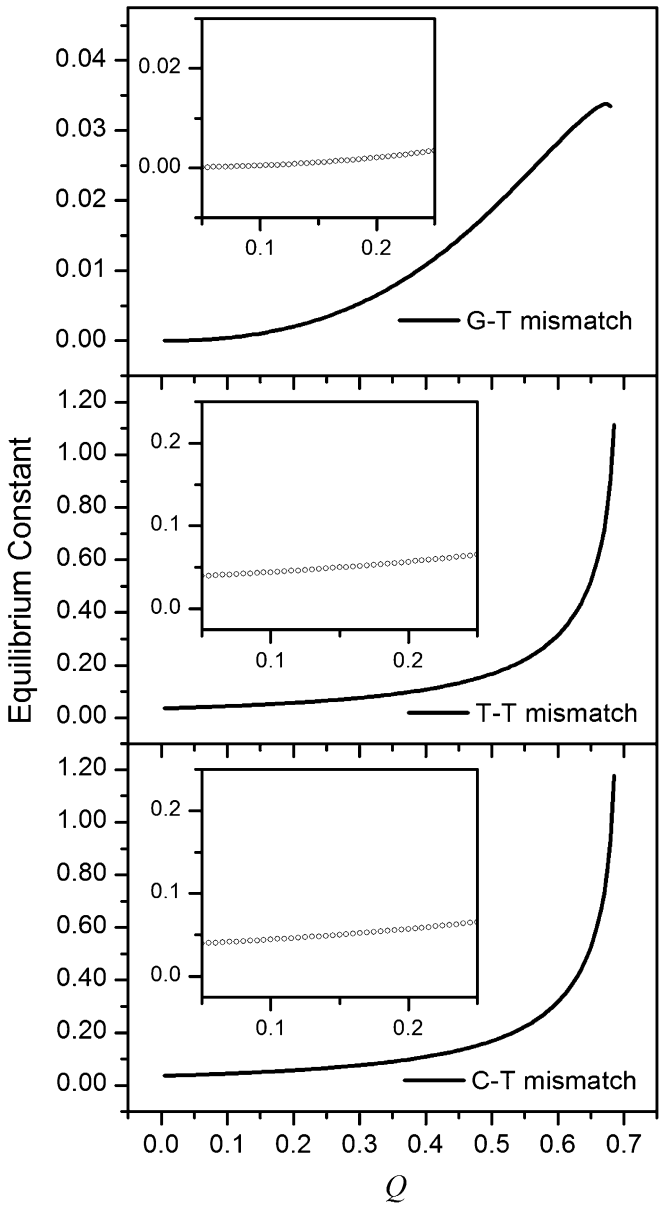

Fig. S5. Dependence of calculated equilibrium constants (K_{open}) of the three tested mismatches on the relative brightness of the flipped-out state at 32.5 °C. (*Inset*) Expanded view of the curve. α was experimentally obtained through fit of G_{flip} of each mismatch.

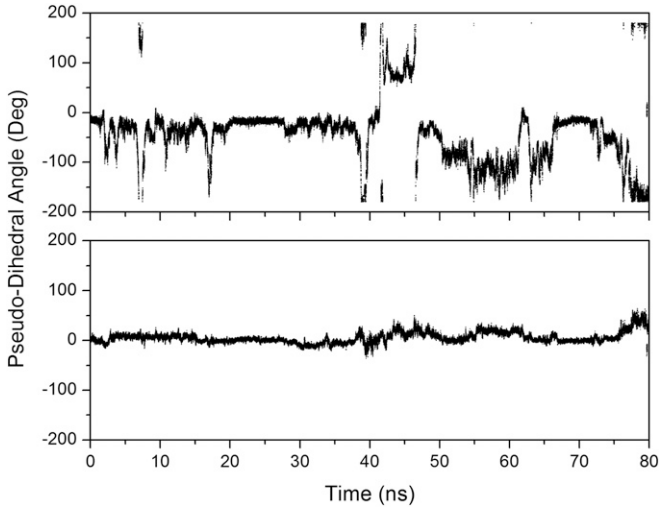

Fig. S6. Pseudodihedral angle (CPDb) changes when SITS is applied to the base T in the G–T mismatch. (*Upper*) CPDb variations of the base T. (*Lower*) CPDb variations of the base G.

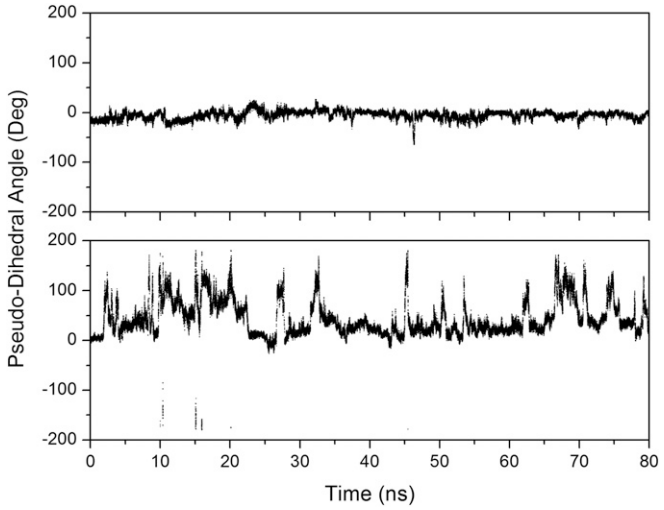

Fig. S7. Pseudodihedral angle changes when SITS is applied to the base G in the G–T mismatch. (*Upper*) CPDb variations of the base T. (*Lower*) CPDb variations of the base G.

Table S1. DNA sequences used in present work

DNA	Sequence
A–T match (dsDNA)	5′-biotin-TTTTTTTTTTCTTCCTCTATTAATATTTACCTCCATTTATAATTA-3′ 3′-GAAGGAGATAATTATAAATGGAGGTAAATATTAAT-5′
G–C match (dsDNA)	5′-biotin-TTTTTTTTTTCTTCCTCTATTAATATTTACCCCCATTTATAATTA-3′ 3′-GAAGGAGATAATTATAAATGGGGGTAAATATTAAT-5′
C–T mismatch (dsDNA)	5′-biotin-TTTTTTTTTTCTTCCTCTATTAATATTTACCTCCATTTATAATTA-3′ 3′-GAAGGAGATAATTATAAATGGCGGTAAATATTAAT-5′
G–T mismatch (dsDNA)	5′-biotin-TTTTTTTTTTCTTCCTCTATTAATATTTACCTCCATTTATAATTA-3′ 3′-GAAGGAGATAATTATAAATGGGGGTAAATATTAAT-5′
T–T mismatch (dsDNA)	5′-biotin-TTTTTTTTTTCTTCCTCTATTAATATTTACCTCCATTTATAATTA-3′ 3′-GAAGGAGATAATTATAAATGGTGGTAAATATTAAT-5′
N–T mismatch* (dsDNA)	5′-biotin-TTTTTTTTTTCTTCCTCTATTAATATTTACCTCCATTTATAATTA-3′ 3′-GAAGGAGATAATTATAAATGG*N*GGTAAATATTAAT-5′
O^{6}meG–C mismatch (dsDNA)	5′-biotin-TTTTTTTTTTCTTCCTCTATTAATATTTACCCCCATTTATAATTA-3′ 3′-GAAGGAGATAATTATAAATGG(O^{6}meG)GGTAAATATTAAT-5′
O^{6}meG–T mismatch (dsDNA)	5′-biotin-TTTTTTTTTTCTTCCTCTATTAATATTTACCTCCATTTATAATTA-3′ 3′-GAAGGAGATAATTATAAATGG(O^{6}meG)GGTAAATATTAAT-5′
TMR-termi (dsDNA)	5′-ATTTATTTATATTTATTTTA-3′ 3′-TAAATAAATATAAATAAAAT-5′
ssT (ssDNA)	5′-biotin-TTTTTTTTTTCTTCCTCTATTAATATTTACCTCCATTTATAATTA-3′
ssC (ssDNA)	5′-biotin-TTTTTTTTTTCTTCCTCTATTAATATTTACCCCCATTTATAATTA-3′
dodecamer† (dsDNA)	5′-TTACC*T*CCATT-3′ 3′-AATGG*X*GGTAA-5′

Underlined nucleotides were labeled with TMR (Fig. S1).
**N* is the abasic nucleotide (Fig. S1).
†Used in the molecular dynamics simulation. The italic *T–X* is a pair of T–T or T–G mismatch.

Table S2. Kinetic parameters of spontaneous flipping of mismatched base pair at $T = 25.0 \pm 0.2$ °C

DNA	K	$k_{\text{flip-in}}$, s^{-1}	$k_{\text{flip-out}}$, s^{-1}	τ_{out}, s	τ_{in}, s
T–T*	$(4.5 \pm 0.8) \times 10^{-2}$	43 ± 10	2.0 ± 0.6	$(23 \pm 5) \times 10^{-3}$	0.51 ± 0.15
C–T	$(3.4 \pm 0.8) \times 10^{-2}$	42 ± 7	1.4 ± 0.4	$(24 \pm 4) \times 10^{-3}$	0.70 ± 0.20
O^{6}meG–T†	$(12.5 \pm 0.3) \times 10^{-4}$	$(1.7 \pm 0.1) \times 10^{2}$	0.22 ± 0.02	$(5.8 \pm 0.4) \times 10^{-3}$	4.6 ± 0.3
G–T	$(3.0 \pm 0.1) \times 10^{-4}$	$(1.2 \pm 0.2) \times 10^{2}$	0.030 ± 0.001	$(10 \pm 2) \times 10^{-3}$	33 ± 7
O^{6}meG–C	$(3.7 \pm 0.2) \times 10^{-4}$	33 ± 7	0.012 ± 0.003	$(30 \pm 6) \times 10^{-3}$	81 ± 17

K is the equilibrium constant for outward flipping of mismatched base pairs. $k_{\text{flip-in}}$ and $k_{\text{flip-out}}$ stand for in- and outward base-flipping rate constants, respectively. $\tau_{\text{out}} = 1/k_{\text{flip-in}}$ and $\tau_{\text{in}} = 1/k_{\text{flip-out}}$ are the lifetimes of the flipping base staying in the extrahelical and intrahelical positions, respectively.
*Errors for T–T, C–T, and G–T mismatches are propagated from that of α and τ_{flip} (mean ± SD, $n = 3$).
†Errors for O^{6}meG–T and O^{6}meG–C mismatches are propagated from that of α and τ_{flip}. The errors of α and τ_{flip} were estimated using a bootstrapping strategy (1).

1. Varian H (2005) Bootstrap tutorial. *The Mathematica Journal* 9:768–775.

Table S3. Energetic parameters of spontaneous flipping of mismatched base pair

DNA	ΔG (kcal/mol)*	ΔH (kcal/mol)†	ΔS (cal/mol/K)	$E_{a,\text{flip-in}}$ (kcal/mol)‡	$E_{a,\text{flip-out}}$ (kcal/mol)§
G-T mismatch	4.66 ± 0.04	7.5 ± 2.2	9.1 ± 7.4	3.1 ± 1.8	10.6 ± 2.8
T–T mismatch	1.89 ± 0.08	0.6 ± 1.5	-4.2 ± 4.9	5.9 ± 0.8	6.5 ± 1.7
C–T mismatch	1.89 ± 0.04	5.9 ± 0.3	13.0 ± 1.1	9.8 ± 2.5	15.6 ± 2.5

*ΔG is at $T = 32.5 \pm 0.2$ °C and is given by $\Delta G = -RT\ln K$, where K is the equilibrium constant (mean± SD, $n = 3$).
†ΔH and ΔS are given by the fit of the equilibrium constant as a function of temperature according to the van't Hoff equation, $-RT\ln K = \Delta G = \Delta H - T\Delta S$, in which ΔH and ΔS are assumed temperature-independent. Errors are given by fit errors.
‡$E_{a,\text{flip-in}}$ is the apparent active energy for the base flipping back to the intrahelical conformation and given by the fit of $k_{\text{flip-in}}$ as a function of temperature according to the Arrhenius equation, $-RT\ln k_{\text{flip-in}} = E_{a,\text{flip-in}} - RT\ln A$, in which $E_{a,\text{flip-in}}$ and the preexponential factor A are assumed temperature-independent. Errors are given by fit errors.
§$E_{a,\text{flip-out}}$ is given by $E_{a,\text{flip-out}} = E_{a,\text{flip-in}} + \Delta H$. Errors are propagated from that of $E_{a,\text{flip-in}}$ and ΔH. A direct fit from $k_{\text{flip-in}}$ according to the Arrhenius equation gave, within the experimental error, the same $E_{a,\text{flip-out}}$ shown here.